MRS Communications (2017), 7, 20–26
© Materials Research Society, 2016
doi:10.1557/mrc.2016.63

MRS Communications

Functional Oxides Prospective Article

Self-assembly of nanostructures with multiferroic components using nucleic acid linkers

Ferman A. Chavez, Department of Chemistry, Oakland University, Rochester, MI 48309-4401, USA
Gopalan Srinivasan, Department of Physics, Oakland University, Rochester, MI 48309-4401, USA
Address all correspondences to either F. A. Chavez at **chavez@oakland.edu** or G. Srinivasan at **srinivas@oakland.edu**

(Received 15 June 2016; accepted 9 December 2016)

Abstract

Self-assembly of multiferroic oxide composites by chemical and biochemical methodology is discussed. The approach involves covalently attaching organic functional groups or oligomeric DNA/RNA to the nanoparticles (NPs). The organic functional groups are only reactive toward functional groups located on different NPs. Using oligomeric DNA/RNA, one could program NPs to only interact with particles possessing complementary DNA/RNA. We have applied both concepts to the assembly of nanostructures with ferrites for the ferromagnetic phase and barium titanate for the ferroelectric phase. The assembled core–shell particles and superstructures obtained in a magnetic field show evidence for strong interactions between the magnetic and ferroelectric subsystems.

Introduction

There is currently an urgent need to establish principles for the assembly of materials with specialized functions/properties at the nanoscale. Construction of nanocomposites with varying architectures and properties can have a wide variety of applications. The development of a theoretical framework for these assemblies is dependent on experimental results, which are needed to establish principles and generalize methodologies.[1,2] The assembly of such materials are far-reaching and are usually approached using two methods[1,3]: the "top-down" and "bottom-up" methods. In the "top-down" approach nanofabrication tools are employed to create nanoscaled structures with targeted shapes and properties beginning with larger structures and reducing them to the desired scale. One example of this approach is lithography. The "bottom-up" method aims to control material at the molecular or atomic level and build complex assemblies at the nanoscale. This approach relies on directed self-assembly based on mechanisms, which are currently under development.[1–8] The bottom-up approach in principle is more efficient than the top-down approach since it is controlled by thermodynamic properties and not by manipulation. Careful design of building blocks and employment of external stimuli such as magnetic/electric fields, gravity, chemical reactivity, temperature, concentration, pH, reaction time, and light to influence assembly allows for the generation of macroscopic materials with high complexity. The employment of reversible processes to create these materials would be ideal since any errors could easily be corrected. There are virtually an infinite number of structural and morphological types that can be generated using this approach. Nanomaterial morphologies (e.g., shapes and surface structures) and distance-dependent properties (e.g., plasmonic and quantum confinement effects), make nanomaterials ideal for future applications, including catalysis, photonics, environmental detection, biomedical diagnostics, and therapy.[2,8,9] Fine control over interactions between nanoparticles (NPs) and composition are critical elements for the construction of these materials. It is additionally anticipated that structures exceeding 100 μm can be produced using nanometer-building blocks, thus making them ideal for incorporation into lithographically produced devices.[2]

Pershina et al., in a recent review discussed the utility of DNA for assembly of magnetic nanoparticles (MNPs) for nanobiocomposites and nanobioelectronics.[3] They addressed interaction of DNA with metallic MNPs as well as magnetic oxides such as Fe_3O_4. Interactions of metal ions could occur with different sites of DNA and are dependent on the nature of metal ions. Alkali-metal ions, in general, form bonds with the phosphate groups, whereas transition metal ions bind to phosphate groups and also to DNA bases. In the case of oxide MNPs such as Fe_3O_4, it was found that the bonding to DNA was through the formation of Fe–O–P bonds.[3] One could, therefore, utilize direct grafting of DNA followed by DNA hybridization to assemble a variety of functional materials and composites, including ferrite–ferroelectric core–shell particles such as $NiFe_2O_4$–$BaTiO_3$ or $CoFe_2O_4$–$BaTiO_3$.[4–8] In this study, however, the assembly procedure involves first functionalizing DNA and NPs with complementary chemical groups, alkyne and azide groups, respectively, in order to attach DNA to NPs by click reaction. This is followed by the assembly of core–shell NPs by DNA hybridization. This procedure is not specific to the systems studied here and could be employed for assembly of a variety of oxide or metal composites.

https://doi.org/10.1557/mrc.2016.63 Published online by Cambridge University Press

Multiferroic nanocomposites

One application of engineered nanomaterials is in the study of multiferroics. A multiferroic is a material that exhibits two or more of the primary ferroic properties (ferromagnetism, ferroelectricity, and ferroelasticity).[10–15] A composite made of a ferromagnetic and ferroelectric material allows for the coupling between the electric and magnetic order parameters (Fig. 1) and represents an engineered multiferroic. The magnetoelectric (ME) coupling is mediated by mechanical forces. When an ac magnetic field is applied to a ferromagnetic material, it oscillates (in size) due to magnetostriction. When this mechanical deformation is transferred to a ferroelectric/piezoelectric material (e.g., PZT and quartz crystal) it responds by producing an electric field due to the piezoelectric effect. Thus, the mechanical strain on these materials produces a magnetic field–electric field conversion. Generation of these composites provides the opportunity for studies on the physics of ME coupling, and have enormous potential for the design of novel miniature functional devices.[11] Such devices include multiple-state logic memories or electrically written magnetic memories, spintronic non-volatile memories, magnetic/electric field sensors, transformers, gyrators, resonators, phase shifters, filters, tunable microwave and optical devices, and antennas.[10,11]

Chemical assembly

Our studies on ferromagnetic–ferroelectric composites revealed a giant low-frequency ME effect and enhancement at electromechanical and ferromagnetic resonance. We also developed theoretical models for the ME phenomena.[10] The strain-mediated ME coupling in core–shell nanocomposites assemblies of ferroelectric (barium titanate, BTO) and ferromagnetic (nickel ferrite, NFO) materials is expected to be very strong due to a surface-to-volume ratio that is a factor of 10^3–10^6 higher than for bulk and thick/film composites. Core–shell NPs of 10–400 nm NFO and 50–600 nm BTO were assembled by attaching complementary chemical groups, azide and alkyne, to particles and then assembling them by the click reaction as shown in Fig. 2.

Studies by scanning electron microscopy (SEM), transmission electron microscopy (TEM), and scanning microwave microscopy (SMM) at 1–26 GHz showed the core–shell structures with well-defined interfaces (Fig. 3).[16–20] Magnetic and ferroelectric characterization revealed ferromagnetic ordering for NFO particles and ferroelectric nature for BTO. We have generalized the method for attaching the groups to the NPs so that any organic group can be attached. This technique is very effective in creating covalent attachments between NFO and BTO NPs and is not limited by the diameters for these particles. A shortcoming, however, is that the attachments are non-dynamic (cannot be reorganized once assembled) and create nanocomposites that are limited in size, which may be due to low coupling efficiency for the click reaction.

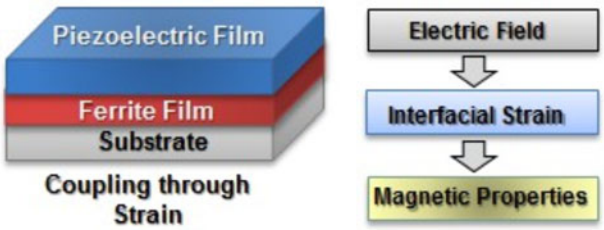


Figure 1. Electric field control of electromagnetic properties of a ferrite–piezoelectric material. The control is through mechanical forces.

DNA-assisted assembly of multiferroic nanocomposites

The use of DNA in the NP self-assembly process has proven to be one of the most versatile methods to date for creating nanostructures of varying structures and compositions.[8,21,22] To accomplish this, DNA is conjugated to nanomaterial/particles via modified functional groups on the custom-synthesized DNA strand. Such groups include sulfhydryl, amine, carboxylate, azide, alkyne, and others located at either the 5′ or 3′ end.[8,23–25] Methods for covalently attaching single-stranded DNA (ssDNA) to NP surfaces have included gold–thiolate interaction,[26–28] Michael addition,[29] disulfide bond formation,[30–32] phosphate–amino linkage via carbodiimide activation,[33] amide bond formation,[34–38] Schiff-base formation,[39] glutaraldehyde-assisted cross-linking,[40–43] and cross-linking using compounds containing sulfhydryl and amino-(N-hydroxysuccinimide) groups.[44–47] The commercial availability of custom-synthesized DNA/RNA containing up to 100 bp with any desired sequence and several 5′ or 3′ organic functional groups offers a great opportunity to explore the effect of sequence and method the attachment. Employment of DNA to assemble NP via hybridization into superlattices has been an example of particle-to-materials fabrication.[48–50] With biologic assemblies many length-scales are crossed using a structural hierarchy. Recently a class of intercalators, $[Ru(dipyrido[2,3\text{-}a\text{:}3',2'\text{-}c]phenazine)\ (N{-}N)_2]^{2+}$-synthesized with DNA was found to increase the bond strength between DNA and NPs.[51] Although work with the employment of DNA as a linker has been reported, essentially no work has been published using RNA.

The Cu(I)-catalyzed azide–alkyne cycloaddition (CuAAC) “click” reaction has also been employed to achieve attachment of DNA to NPs.[52–54] Recent work by Mirkin and co-workers has demonstrated that alkyne-functionalized ssDNA can be bound to NPs via CuAAC “click” chemistry yielding NPs with high-density monolayers of DNA on the surface.[52] In their work, they attach single-stranded oligomeric DNA to superparamagnetic iron oxide nanoparticles as a proof-of-concept study. In our work, 3-buten-1-ol was grafted to the surfaces of 600 nm BTO and 200 nm NFO using 254 nm light under anaerobic conditions. These groups were subsequently converted to alkyl–azide groups (Fig. 2 top) and alkyne-functionalized DNA (custom synthesized by Keck Laboratories, Inc.) was attached via the click reaction.[55]

https://doi.org/10.1557/mrc.2016.63 Published online by Cambridge University Press

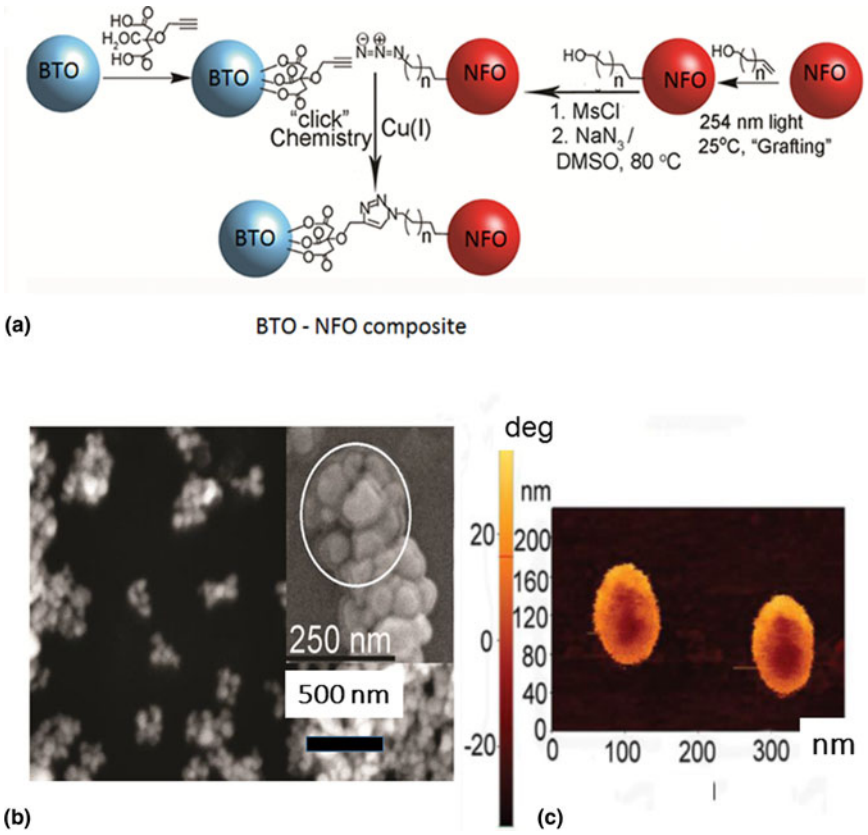


Figure 2. (top) Synthesis of BTO and NFO core–shell NPs by chemical self-assembly: particles were functionalized with complementary coupling groups (propargyl and azide groups) and then assembled in the presence of copper catalyst. (bottom left) SEM of core–shell particle. (bottom left, inset) SEM of collection of core–shell particles. (bottom right) MFM phase image showing the core–shell structure.[16–20]

RNA-assisted assembly of multiferroic nanocomposites

RNA-based nanotechnology is a newly emerging field.[56–59] There has been an increasing interest in RNA for the assembly of nanostructures over the past few years as indicated by the increase in publications. Compared with DNA, RNA possesses higher thermodynamic stability, a higher variety of base-pairing alternatives, and programmable tertiary structure formation (helices, stems, loops, hairpins, bulges, and pseudoknots).[56] The known degradation of RNA from RNase enzymes has previously caused scientists to avoid employing RNA in nanotechnology. This has resulted in disinterest in this field. Assuming that this remains a problem with oligomeric RNA, one could use alternative strategies to generate degradation-resistant RNA.[60] Improvements in stability could come from using modified bases (i.e., 5-Br-U, 5-I-U), modified phosphate linkages (i.e., phosphothiolate, boranophosphate), peptide nucleic acids (i.e., PNA), or C2′ modifications (i.e., 2′-fluorine, 2′-O-methyl, or 2′-O-amine).[56,58] Using computer-designed oligonucleotide RNA, Jaeger and co-workers were able to generate three-dimensional (3D) nanoscaffolds that assembled in vitro.[61] Other 3D structures have been assembled using similar techniques.[62] Due to the great diversity of base-pair and folding interactions with RNA, computer programs have been developed to help predict 3D structures.[63,64] NP formation of modified RNA via metal (i.e., Fe and Co) complexation has also been reported.[59]

Formation of ordered structures by magnetic fields

One of the key objectives of our research is to assemble nanomaterials into superstructures, which are predicted to exhibit strong ME coupling at low frequencies and resonance ME effects over a wide frequency range of interest. The procedure involves heating the nanomaterials in a solution to 80 °C for dehybridization, followed by cooling under a field so that DNA-assisted assembly and field-directed assembly occur simultaneously. The set ups as in Fig. 4 are useful for assembly under magnetic and electric fields.[65,66] The uniformity, position, and patterns can be controlled with positioning or patterning of magnets on a substrate or the frequency and amplitude of applied voltage. Our efforts toward *H*-assembly of superstructures have been successful. Figure 4 shows SEM images of

https://doi.org/10.1557/mrc.2016.63 Published online by Cambridge University Press

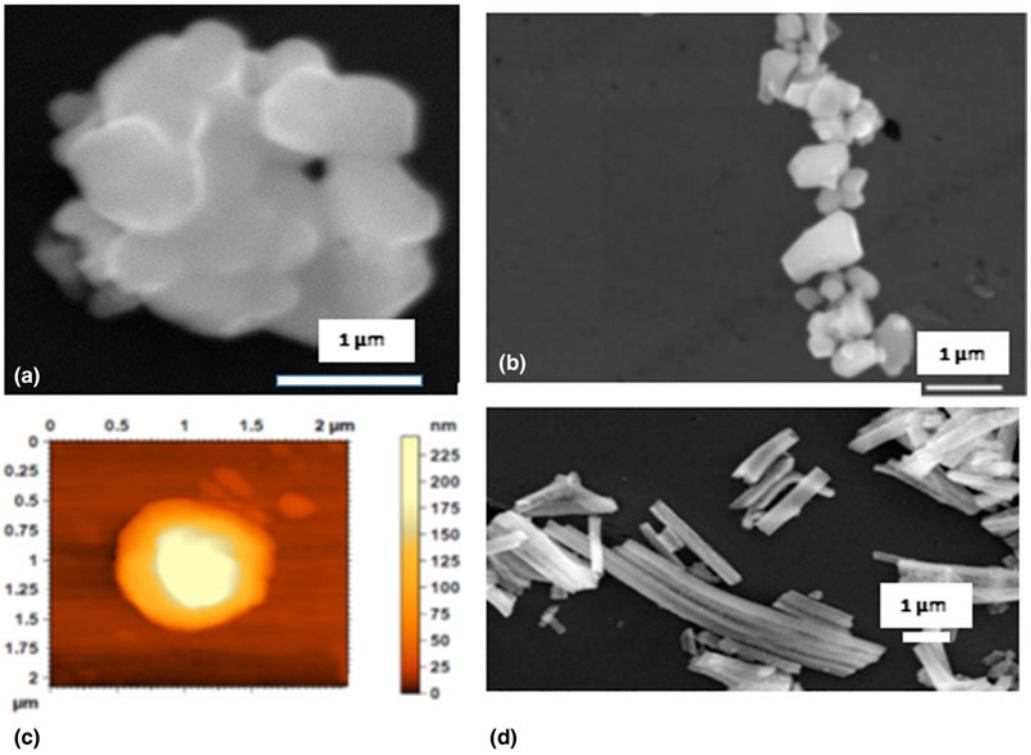


Figure 3. (a) SEM image showing a DNA-assembled particle of 600 nm BTO core–200 nm NFO shell. (b) SEM image of an array of core–shell particles assembled under a magnetic field. (c) SMM topography image of the particle. (d) SEM of bundle of ferrite-PZT core–shell nanowires assembled with DNA.

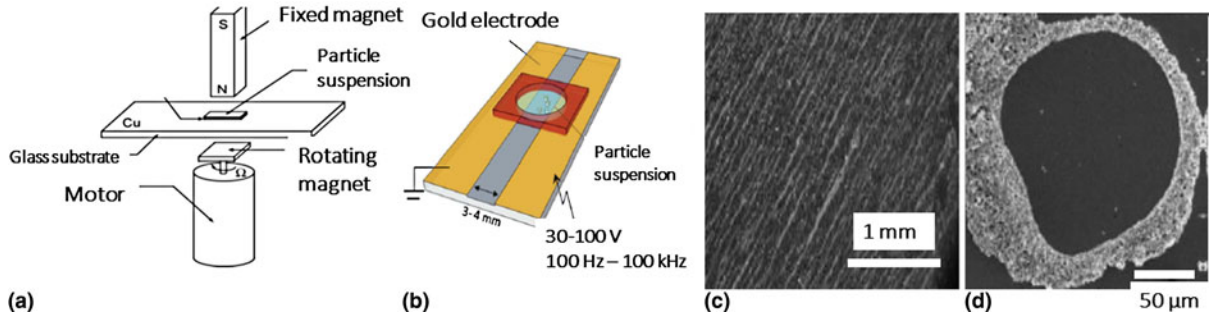


Figure 4. (a) A setup for *H*-assisted assembly. Binding site is a substrate with patterned Ni/permalloy bottom and assists in assembly of desired structure for core–shell or coaxial tubes/wires.[65] (b) *E*-field-assisted assembly set up.[66] (c) SEM image showing a 2.5 × 2.5 mm^2 2D superstructure of 600 nm BTO and 200 nm NFO core–shell particles obtained in a uniform *H*-field. (d) A ring of the core–shell particles assembled in a rotating magnetic field.

2.5 × 2.5 mm^2 array and a ring of DNA-assembled core–shell particle obtained with uniform and rotating fields, respectively.

Magnetic, ferroelectric, and multiferroic properties of assembled composites

It is essential to characterize the DNA-assembled composites and superstructures in terms of ferroic order parameters and ME coupling strength.[55,67,68] The ferromagnetic properties of the composite was studied by measurements of room-temperature magnetization *M* as a function of the static magnetic field *H*. Figure 5(a) shows such date for the core–shell composite and a ferromagnetic character is clearly evident from the data. The magnetization shows saturation value of 17.5 emu/g for $H \sim 2.5$ kOe, which is about 60% of the value expected for the bulk NFO-only sample. The ferroelectric nature of the composites was confirmed with polarization *P* versus electric field *E* measurements with a (Radiant Technology) ferroelectric tester. The data in Fig. 5(b) indicate remnant polarization of 4 mC/m^2 and a saturation value of

https://doi.org/10.1557/mrc.2016.63 Published online by Cambridge University Press

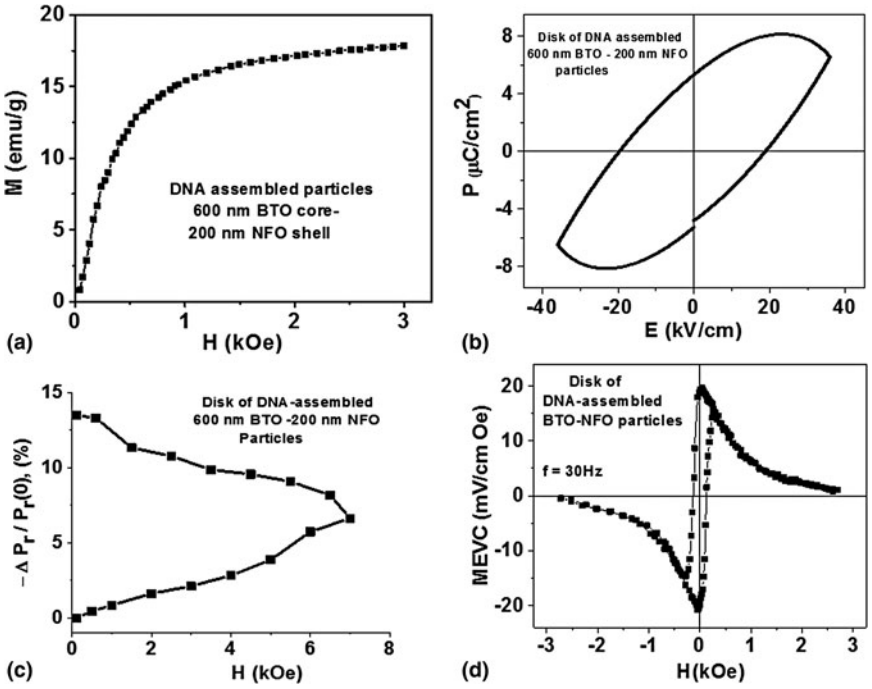


Figure 5. (a) Room-temperature magnetization as a function of static magnetic field for as-assembled BTO–NFO composite. (b) Polarization *P* versus electric field *E* data for a disc of DNA-assembled BTO–NFO core–shell particles. (c) Fraction change in the remnant polarization P_r versus *H* obtained from data as in Fig. 5 (b) when the sample is subjected to an in-plane static magnetic field. (d) Low-frequency MEVC versus *H* for a sintered disc of DNA-assembled BTO–NFO particles.[55]

~8 mC/m^2, values that are somewhat smaller than values reported for the bulk or thick film BTO.

Magneto-electric characterization of the composites could be done by measuring the sample response to: (i) an applied magnetic field (termed direct-ME effect) and (ii) an applied electric field (converse ME effect). Here we provide results on the direct-ME effect by two different techniques: static magnetic field *H*-induced polarization *P* in the sample and low-frequency ME voltage coefficient. Measurements were first carried out on pressed pellets of as-assembled core–shell composites. Figure 5(c) shows the results on direct-ME effect (DME) by static magnetic field *H*-induced polarization through *P* versus *E* measurements in a disc of DNA-assembled sample. The samples were subjected to a uniform in-plane magnetic field. A decrease in *P* due to *H* was measured. The fractional change in the remnant polarization $\Delta P_r/P_r\ (H=0) = [P_r(H) - P(H=0)]/P_r\ (H=0)$ versus *H* measured from *P* versus *E* for *H* = 0–7 kOe are shown. As *H* is increased from 0 to 7 kOe, $\Delta P_r/P_r$ increases with *H* to ~7% at *H* = 7 kOe. When *H* is decreased back to zero, a hysteresis is seen in $\Delta P_r/P_r$ versus *H* with the magnitude $\Delta P_r/P_r$ increasing to 13% for *H* = 0. Thus, the results in Fig. 5(c) provide clear evidence for magnetostriction-induced change in polarization for the composite.[55]

We also studied the nature of DME by low-frequency ME voltage coefficient (MEVC) measurements on sintered discs of DNA-assembled sample. The samples were first poled in *E* = 1 kV/cm at room temperature and then subjected to a dc bias magnetic field *H* and an ac field of H_{ac} = 1 Oe at 30 Hz. The ac and dc magnetic fields were parallel to each other and applied parallel to the disc plane. The ME voltage induced across the disc thickness was measured as a function of *H*. Figure 5(d) shows MEVC versus *H* data for the DNA-assembled sample. The MEVC shows a zero-bias (*H* = 0) value of 20 mV/cm Oe and is indicative of a built-in magnetic field arising from dipole–dipole interactions between NFO particles in the core–shell structures. With increase in *H*, MEVC decreases and the coupling vanishes at *H* = 2 kOe due to saturation of magnetostriction resulting in zero value for the piezomagnetic coupling *q*. A hysteresis is also seen in MEVC versus *H* data. When *H* is reversed the MEVC becomes negative (a 180° phase difference with H_{ac}). For comparison we measured MEVC on thin discs of the composites made by mixing NFO and BTO particles. The MEVC was much smaller than for DNA-assembled samples. For our DNA-assembled nanocomposites, we observed strong ME coupling in as-assembled composites, which is evident from polarization induced by magnetic field *H* and MEVC results in Fig. 5. We found that annealing the samples at high temperatures removes the organic components and enhances the interaction of the components yielding excellent ME coupling evident by low-frequency ME voltage coefficient and *H*-induced polarization.[55]

Composites with a ferrite core and BTO or lead zirconate titanate (PZT) shell can also be synthesized by a two-step hydrothermal and annealing process or a surfactant-assisted thermal

https://doi.org/10.1557/mrc.2016.63 Published online by Cambridge University Press

method.[69,70] Several systems, including $Fe_3O_4/PbTiO_3$, $CoFe_2O_4/BaTiO_3$, and $CoFe_2O_4/Pb(Zr,Ti)O_3$ were synthesized. The synthesis technique facilitated control over size of the core and thickness of shell.[69] Measurements of ME coupling strength by magnetodielectric effect was reported for $CoFe_2O_4/BaTiO_3$. The dielectric constant at 134 K decreased by 1.7% for an applied field of 10 kOe.[70] Thus, one infers that the ME coupling in the composite is much weaker than the measured coupling strength in the DNA-assembled core–shell particles (Fig. 5). It is quite clear that assembling the nanocomposites using the DNA-assisted method followed by sintering affords materials with superior ME coupling strengths.[55]

Conclusions and outlook

Most of the work involving DNA-attachment to NPs has focused on noble metals such as gold and thiol-tethered DNA. The attachment of programmable nucleic acid oligomers to metal oxide NPs is new and provides them with smart properties enabling them to seek out interactions via DNA/RNA–DNA/RNA hybridization. Incorporation of these modifications to multiferroic precursors is a newly emerging field and may hold promise in the design of material structure and properties at the nanoscale.

Acknowledgements

We gratefully acknowledge help by Drs. Sreenivasulu Gollapudi and Manashi Panda in sample synthesis and characterization. The research was supported by a grant from the Army Research Office (grant no: W911NF1210545). The efforts were also supported in part by grants from the National Science Foundation (grant numbers DMR-0902701, ECCS-1040304, ECCS-1337716, CHE-0748607, and CHE-0821487).

References

1. A. Biswas, I.S. Bayer, A.S. Biris, T. Wang, E. Dervishi, and F. Faupel: Advances in top-down and bottom-up surface nanofabrication: techniques, applications and future prospects. *Adv. Colloid Interface Sci.* **170**, 2 (2012).
2. L.G. Xu, W. Ma, L.B. Wang, C.L. Xu, H. Kuang, and N.A. Kotov: Nanoparticle assemblies: dimensional transformation of nanomaterials and scalability. *Chem. Soc. Rev.* **42**, 3114 (2013).
3. A.G. Pershina, A.E. Sazonov, and V.D. Filimonov: Magnetic nanoparticles–DNA interactions: design and applications of nanobiohybrid systems. *Russ. Chem. Rev.* **83**, 299 (2014).
4. N.Z. Bao and A. Gupta: Self-assembly of superparamagnetic nanoparticles. *J. Mater. Res.* **26**, 111 (2011).
5. S.J. Barrow, A.M. Funston, X.Z. Wei, and P. Mulvaney: DNA-directed self-assembly and optical properties of discrete 1D, 2D and 3D plasmonic structures. *Nano Today* **8**, 138 (2013).
6. M.H. Huang and S. Thoka: Formation of supercrystals through self-assembly of polyhedral nanocrystals. *Nano Today* **10**, 81 (2015).
7. H.Y. Li, J.D. Carter, and T.H. LaBean: Nanofabrication by DNA self-assembly. *Mater. Today* **12**, 24 (2009).
8. L.H. Tan, H. Xing, and Y. Lu: DNA as a powerful tool for morphology control, spatial positioning, and dynamic assembly of nanoparticles. *Acc. Chem. Res.* **47**, 1881 (2014).
9. A. Schroeder, D.A. Heller, M.M. Winslow, J.E. Dahlman, G.W. Pratt, R. Langer, T. Jacks, and D.G. Anderson: Treating metastatic cancer with nanotechnology. *Nat. Rev. Cancer* **12**, 39 (2012).
10. C.W. Nan, M.I. Bichurin, S.X. Dong, D. Viehland, and G. Srinivasan: Multiferroic magnetoelectric composites: historical perspective, status, and future directions. *J Appl. Phys.* **103**, 031101 (2008).
11. N.X. Sun and G. Srinivasan: Voltage control of magnetism in multiferroic heterostructures and devices. *SPIN* **02**, 124004 (2012).
12. G. Schileo: Recent developments in ceramic multiferroic composites based on core/shell and other heterostructures obtained by sol-gel routes. *Progr. Solid State Chem.* **41**, 87 (2013).
13. F.M. Bai, H.W. Zhang, J.F. Li, and D. Viehland: Magnetic and magnetoelectric properties of as-deposited and annealed $BaTiO_3$–$CoFe_2O_4$ nanocomposite thin films. *J. Phys. D: Appl. Phys.* **43**, 285002 (2010).
14. C. Brosseau, V. Castel, and M. Potel: Controlled extrinsic magnetoelectric coupling in $BaTiO_3$/Ni nanocomposites: effect of compaction pressure on interfacial anisotropy. *J. Appl. Phys.* **108**, 024306 (2010).
15. H.M. Wang, E. Pan, and W.Q. Chen: Large multiple resonance of magnetoelectric effect in a multiferroic composite cylinder with an imperfect interface. *Phys. Status Solidi B* **248**, 2180 (2011).
16. G. Sreenivasulu, M. Popov, F.A. Chavez, S.L. Hamilton, P.R. Lehto, and G. Srinivasan: Controlled self-assembly of multiferroic core–shell nanoparticles exhibiting strong magneto-electric effects. *Appl. Phys. Lett.* **104**, 052901 (2014).
17. M. Popov, G. Sreenivasulu, V.M. Petrov, F.A. Chavez, and G. Srinivasan: High frequency magneto-dielectric effects in self-assembled ferrite–ferroelectric core–shell nanoparticles. *AIP Adv.* **4**, 097117 (2014).
18. G. Sreenivasulu, V.M. Petrov, F.A. Chavez, and G. Srinivasan: Superstructures of self-assembled multiferroic core–shell nanoparticles and studies on magneto-electric interactions. *Appl. Phys. Lett.* **105**, 072905 (2014).
19. G. Srinivasan, M. Popov, G. Sreenivasulu, V.M. Petrov, and F.A. Chavez: Millimeter-wave magneto-dielectric effects in self-assembled ferrite–ferroelectric core–shell nanoparticles. *J. Appl. Phys.* **117**, 17A309 (2015).
20. G. Srinivasan, G. Sreenivasulu, C. Benoit, V.M. Petrov, and F. Chavez: Magnetic field directed assembly of superstructures of ferrite-ferroelectric core–shell nanoparticles and studies on magneto-electric interactions. *J. Appl. Phys.* **117**, 17B904 (2015).
21. Y. Guo, Y. Hu, and Z.T. Deng: DNA directed self-assembly of fluorescent colloidal semiconductor quantum dots and plasmonic metal nanoparticles heterogeneous nanomaterials. *Chin. J. Chem.* **34**, 259 (2016).
22. Y.R. Ma, X.D. Yang, Y.R. Wei, and Q. Yuan: Applications of DNA nanotechnology in synthesis and assembly of inorganic nanomaterials. *Chin. J. Chem.* **34**, 291 (2016).
23. H. Ravan, S. Kashanian, N. Sanadgol, A. Badoei-Dalfard, and Z. Karami: Strategies for optimizing DNA hybridization on surfaces. *Anal. Biochem.* **444**, 41 (2014).
24. L.L. Li, P.W. Wu, K. Hwang, and Y. Lu: An exceptionally simple strategy for DNA-functionalized up-conversion nanoparticles as biocompatible agents for nanoassembly, DNA delivery, and imaging. *J. Am. Chem. Soc.* **135**, 2411 (2013).
25. A. Kumar, J.H. Hwang, S. Kumar, and J.M. Nam: Tuning and assembling metal nanostructures with DNA. *Chem. Commun.* (*Camb.*) **49**, 2597 (2013).
26. M. Banchelli, S. Nappini, C. Montis, M. Bonini, P. Canton, D. Berti, and P. Baglioni: Magnetic nanoparticle clusters as actuators of ssDNA release. *Phys. Chem. Chem. Phys.* **16**, 10023 (2014).
27. I. Robinson, D. Tung le, S. Maenosono, C. Walti, and N.T. Thanh: Synthesis of core–shell gold coated magnetic nanoparticles and their interaction with thiolated DNA. *Nanoscale* **2**, 2624 (2010).
28. M. Pita, J.M. Abad, C. Vaz-Dominguez, C. Briones, E. Mateo-Marti, J.A. Martin-Gago, P. Morales Mdel, and V.M. Fernandez: Synthesis of cobalt ferrite core/metallic shell nanoparticles for the development of a specific PNA/DNA biosensor. *J. Colloid Interface Sci.* **321**, 484 (2008).
29. N. Kitamura, R. Nakai, H. Kohda, K. Furuta-Okamoto, and H. Iwata: Labeling of islet cells with iron oxide nanoparticles through DNA hybridization for highly sensitive detection by MRI. *Bioorgan. Med. Chem.* **21**, 7175 (2013).

https://doi.org/10.1557/mrc.2016.63 Published online by Cambridge University Press

30. H. Shen, Y. Wang, H. Yang, and J. Jiang: Covalent immobilization of oligo-DNA on the surface of magnetic nanoparticles and surface-enhanced Raman scattering study. *Chin. Sci. Bull.* **48**, 2698 (2003).
31. F. Wang, H. Shen, J. Feng, and H. Yang: PNA-modified magnetic nanoparticles and their hybridization with single-stranded DNA target: surface enhanced Raman scatterings study. *Microchim. Acta* **153**, 15 (2006).
32. S. Santra, R. Yapec, N. Theodoropoulou, J. Dobson, A. Hebard, and W. Tan: Synthesis and characterization of silica-coated iron oxide nanoparticles in microemulsion: the effect of nonionic surfactants. *Langmuir* **17**, 2900 (2001).
33. N. Zhu, A. Zhang, P. He, and Y. Fang: DNA hybridization at magnetic nanoparticles with electrochemical stripping detection. *Electroanalysis* **16**, 1925 (2004).
34. C.D. Medley, J.E. Smith, L.S. Wigman, and N.P. Chetwyn: A DNA-conjugated magnetic nanoparticle assay for assessing genotoxicity. *Anal Bioanal. Chem* **404**, 2233 (2012).
35. K. Wagner, A. Kautz, M. Röder, M. Schwalbe, K. Pachmann, J.H. Clement, and M. Schnabelrauch: Synthesis of oligonucleotide-functionalized magnetic nanoparticles and study on their in vitro cell uptake. *Appl. Organometal. Chem.* **18**, 514 (2004).
36. X. Zhu, X. Zhou, and D. Xing: Nano-magnetic primer based electrochemiluminescence-polymerase chain reaction (NMPE-PCR) assay. *Biosens. Bioelectron.* **31**, 463 (2012).
37. D.B. Robinson, H.H. Persson, H. Zeng, G. Li, N. Pourmand, S. Sun, and S. X. Wang: DNA-functionalized MFe_2O_4 (M = Fe, Co, or Mn) nanoparticles and their hybridization to DNA-functionalized surfaces. *Langmuir* **21**, 3096 (2005).
38. M. Yin, Z. Li, Z. Liu, J. Ren, X. Yang, and X. Qu: Photosensitizer-incorporated G-quadruplex DNA-functionalized magnetofluorescent nanoparticles for targeted magnetic resonance/fluorescence multimodal imaging and subsequent photodynamic therapy of cancer. *Chem. Commun.* **48**, 6556 (2012).
39. M. Fuentes, C. Mateo, A. Rodriguez, M. Casqueiro, J.C. Tercero, H. H. Riese, R. Fernandez-Lafuente, and J.M. Guisan: Detecting minimal traces of DNA using DNA covalently attached to superparamagnetic nanoparticles and direct PCR-ELISA. *Biosens. Bioelectron.* **21**, 1574 (2006).
40. G. Amagliani, E. Omiccioli, A. Campo, I.J. Bruce, G. Brandi, and M. Magnani: Development of a magnetic capture hybridization-PCR assay for Listeria monocytogenes direct detection in milk samples. *J. Appl. Microbiol.* **100**, 375 (2006).
41. J.Y. Lin and Y.C. Chen: Functional magnetic nanoparticle-based trapping and sensing approaches for label-free fluorescence detection of DNA. *Talanta* **86**, 200 (2011).
42. A. del Campo, T. Sena, J.-P. Lellouchec, and I.J. Brucea: Multifunctional magnetite and silica–magnetite nanoparticles: synthesis, surface activation and applications in life sciences. *J. Magn. Magn. Mater.* **293**, 33 (2005).
43. L.B. Nie, X.L. Wang, S. Li, and H. Chen: Amplification of fluorescence detection of DNA based on magnetic separation. *Anal. Sci.* **25**, 1327 (2009).
44. L. Josephson, J.M. Perez, and R. Weissleder: Magnetic nanosensors for the detection of oligonucleotide sequences. *Angew. Chem. Int. Ed. Engl.* **40**, 3204 (2001).
45. M.V. Yigit, D. Mazumdar, H.K. Kim, J.H. Lee, B. Odintsov, and Y. Lu: Smart "turn-on" magnetic resonance contrast agents based on aptamer-functionalized superparamagnetic iron oxide nanoparticles. *Chembiochem.: Eur. J. Chem. Biol.* **8**, 1675 (2007).
46. J. Grimm, J.M. Perez, L. Josephson, and R. Weissleder: Novel nanosensors for rapid analysis of telomerase activity. *Cancer Res.* **64**, 639 (2004).
47. F.W. Osterberg, G. Rizzi, T. Zardan Gomez de la Torre, M. Stromberg, M. Stromme, P. Svedlindh, and M.F. Hansen: Measurements of Brownian relaxation of magnetic nanobeads using planar Hall effect bridge sensors. *Biosens. Bioelectron.* **40**, 147 (2013).
48. S.Y. Park, A.K. Lytton-Jean, B. Lee, S. Weigand, G.C. Schatz, and C. A. Mirkin: DNA-programmable nanoparticle crystallization. *Nature* **451**, 553 (2008).
49. R.J. Macfarlane, M.R. Jones, A.J. Senesi, K.L. Young, B. Lee, J. Wu, and C.A. Mirkin: Establishing the design rules for DNA-mediated programmable colloidal crystallization. *Angew. Chem. Int. Ed. Engl.* **49**, 4589 (2010).
50. F. Lu, K.G. Yager, Y.G. Zhang, H.L. Xin, and O. Gang: Superlattices assembled through shape-induced directional binding. *Nat. Commun.* **6**, 6912 (2015).
51. S.E. Seo, M.X. Wang, C.M. Shade, J.L. Rouge, K.A. Brown, and C. A. Mirkin: Modulating the bond strength of DNA–nanoparticle superlattices. *ACS Nano* **10**, 1771 (2016).
52. J.I. Cutler, D. Zheng, X. Xu, D.A. Giljohann, and C.A. Mirkin: Polyvalent oligonucleotide iron oxide nanoparticle "click" conjugates. *Nano Lett.* **10**, 1477 (2010).
53. D.A. Thomson, E.H. Tee, N.T. Tran, M.J. Monteiro, and M.A. Cooper: Oligonucleotide and polymer functionalized nanoparticles for amplification-free detection of DNA. *Biomacromolecules* **13**, 1981 (2012).
54. C. Kaittanis, H. Boukhriss, S. Santra, S.A. Naser, and J.M. Perez: Rapid and sensitive detection of an intracellular pathogen in human peripheral leukocytes with hybridizing magnetic relaxation nanosensors. *PLoS ONE* **7**, e35326 (2012).
55. G. Sreenivasulu, T.A. Lochbiler, M. Panda, G. Srinivasan, and F.A. Chavez: Self-assembly of multiferroic core–shell particulate nanocomposites through DNA–DNA hybridization and magnetic field directed assembly of superstructures. *AIP Adv.* **6**, 045202 (2016).
56. G.C. Shukla, F. Haque, Y. Tor, L.M. Wilhelmsson, J.J. Toulme, H. Isambert, P. Guo, J.J. Rossi, S.A. Tenenbaum, and B.A. Shapiro: A boost for the emerging field of RNA nanotechnology. *ACS Nano* **5**, 3405 (2011).
57. W.W. Grabow and L. Jaeger: RNA self-assembly and RNA nanotechnology. *Acc. Chem. Res.* **47**, 1871 (2014).
58. A. Sharma, F. Haque, F. Pi, L.S. Shlyakhtenko, B.M. Evers, and P. Guo: Controllable self-assembly of RNA dendrimers. *Nanomed.: Nanotechnol. Biol. Med.* **12**, 835 (2016).
59. C.J. Carter, M. Dolska, A. Owczarek, C.J. Ackerson, B.E. Eaton, and D. L. Feldheim: In vitro selection of RNA sequences capable of mediating the formation of iron oxide nanoparticles. *J. Mater. Chem.* **19**, 8320 (2009).
60. J. Liu, S.C. Guo, M. Cinier, L.S. Shlyakhtenko, Y. Shu, C.P. Chen, G. Shen, and P.X. Guo: Fabrication of stable and RNase-resistant RNA nanoparticles active in gearing the nanomotors for viral DNA packaging. *ACS Nano* **5**, 237 (2011).
61. K.A. Afonin, E. Bindewald, A.J. Yaghoubian, N. Voss, E. Jacovetty, B. A. Shapiro, and L. Jaeger: In vitro assembly of cubic RNA-based scaffolds designed in silico. *Nat. Nanotechnol.* **5**, 676 (2010).
62. W.W. Grabow, P. Zakrevsky, K.A. Afonin, A. Chworos, B.A. Shapiro, and L. Jaeger: Self-assembling RNA nanorings based on RNAI/II inverse kissing complexes. *Nano Lett.* **11**, 878 (2011).
63. N.R. Markham and M. Zuker: UNAFold: software for nucleic acid folding and hybridization. *Methods Mol. Biol.* **453**, 3 (2008).
64. O.V. Matveeva, Y. Kang, A.N. Spiridonov, P. Saetrom, V.A. Nemtsov, A. Y. Ogurtsov, Y.D. Nechipurenko, and S.A. Shabalina: Optimization of duplex stability and terminal asymmetry for shRNA design. *PLoS ONE* **5**, e10180 (2010).
65. D. Wang and H.H. Ko: Magnetic-assisted self-assembly of rectangular shaped parts. *Sens. Actuators* **151**, 195 (2009).
66. S.K. Smoukov, S. Gangwal, M. Marquez, and O.D. Velev: Reconfigurable responsive structures assembled from magnetic Janus particles. *Soft Matter.* **5**, 1285 (2009).
67. J.X. Zhang, J.Y. Dai, C.K. Chow, C.L. Sun, V.C. Lo, and H.L.W. Chan: $CoFe_2O_4/SrRuO_3/Pb(Zr_{0.52}\ Ti_{0.48})O_3CoFe_2O_4/SrRuO_3/Pb(Zr_{0.52}\ Ti_{0.48})O_3$ heteroepitaxial thin film structure. *Appl. Phys. Lett.* **92**, 022901 (2008).
68. J.X. Zhang, J.Y. Dai, W. Lu, and H.L.W. Chan: Room temperature magnetic exchange coupling in multiferroic $BaTiO_3/CoFe_2O_4$ magnetoelectric superlattice. *J. Mater. Res.* **44**, 5143 (2009).
69. R. Liu, Y. Zhao, R. Huang, Y. Zhao, and H. Zhou: Multiferroic ferrite/perovskite oxide core/shell nanostructures. *J. Mater. Chem.* **20**, 10665 (2010).
70. K. Raidongia, A. Nag, A. Sundaresan, and C.N.R. Rao: Multiferroic and magnetoelectric properties of core–shell $CoFe_2O_4$–$BaTiO_3$ nanocomposites. *Appl. Phys. Lett.* **97**, 062904 (2010).

https://doi.org/10.1557/mrc.2016.63 Published online by Cambridge University Press